NUCLEIC ACID THERAPEUTICS
Volume 27, Number 5, 2017

DOI: 10.1089/nat.2017.0686

Induction of RNAi Responses by Short Left-Handed Hairpin RNAi Triggers

Jonathan C. Hagopian,*,† Alexander S. Hamil,* Arjen van den Berg, Bryan R. Meade,‡ Akiko Eguchi,§ Caroline Palm-Apergi,¶ and Steven F. Dowdy

Small double-stranded, left-handed hairpin (LHP) RNAs containing a 5′-guide-loop-passenger-3′ structure induce RNAi responses by a poorly understood mechanism. To explore LHPs, we synthesized fully 2′-modified LHP RNAs targeting multiple genes and found all to induce robust RNAi responses. Deletion of the loop and nucleotides at the 5′-end of the equivalent passenger strand resulted in a smaller LHP that still induced strong RNAi responses. Surprisingly, progressive deletion of up to 10 nucleotides from the 3′-end of the guide strand resulted in a 32mer LHP capable of inducing robust RNAi responses. However, further guide strand deletion inhibited LHP activity, thereby defining the minimal length guide targeting length to 13 nucleotides. To dissect LHP processing, we examined LHP species that coimmunoprecipitated with Argonaute 2 (Ago2), the catalytic core of RNA-induced silencing complex, and found that the Ago2-associated processed LHP species was of a length that correlated with Ago2 cleavage of the passenger strand. Placement of a blocking 2′-OMe blocking modification at the LHP predicted Ago2 cleavage site resulted in an intact LHP loaded into Ago2 and no RNAi response. Taken together, these data argue that in the absence of a substantial loop, this novel class of small LHP RNAs enters the RNAi pathway by a Dicer-independent mechanism that involves Ago2 cleavage and results in an extended guide strand. This work establishes LHPs as an alternative RNAi trigger that can be produced from a single synthesis for potential use as an RNAi therapeutic.

Keywords: RNAi responses, RNAi triggers, left-handed hairpin RNA

Introduction

The discovery of RNA interference (RNAi) in *Caenorhabditis elegans* [1] revealed a novel post-transcriptional mechanism of gene regulation mediated by double-stranded RNA. The combined activity of Drosha and Dicer ribonucleases cleaves and processes long double-stranded RNA hairpin loops into 21–23 nucleotide double-stranded micro-RNAs (miRNAs) with 3′ dinucleotide overhangs that are loaded by TAT RNA binding protein (TRBP) into Argonaute proteins, the catalytic subunit of RNA-induced silencing complex (RISC), to induce RNAi responses [2]. The sense strand or ''passenger'' strand is removed and the antisense or ''guide'' strand remains loaded in the RISC to scan mRNA transcript for target sequences. The ability of exogenously administered synthetic short interfering RNAs (siRNA) 21–23 nucleotides in length with two nucleotide 3′ overhangs to engage the RNAi machinery downstream of Dicer opened the door for performing selective gene silencing [3]. Given the specificity, potency, and ability to target the undruggable genome, siRNA-induced RNAi responses have great potential for treating human disease, particularly cancer with its myriad of genetic mutations [4,5]. Moreover, due to the ability to induce synthetic lethal RNAi responses and to evolve the siRNA ''drug'' as fast as the patient's tumor genetics evolve, RNAi therapeutics stand alone in their potential for development of personalized cancer treatment [6,7].

Beyond siRNA, multiple groups have demonstrated efficacy with alternative RNAi inducing molecular structures, including long double-stranded RNAs [8] and short-hairpin RNAs (shRNAs) that contain large intervening loops based on miRNA stem-loop characteristics, and use DNA-based viral vectors driven by RNA polymerase II or III promoters [9–12]. Several studies investigating the potency of synthetic shRNAs have found combined influences contributed by the stem, loop, and 3′-end structure [11,13]. Interestingly, the

Department of Cellular and Molecular Medicine, UCSD School of Medicine, La Jolla, California.
*These authors contributed equally to this work.
†Current affiliation: Advanced Analytical Technologies Inc., Ankeny, Iowa.
‡Current affiliation: Solstice Biologics, San Diego, California.
§Current affiliation: Department of Gastroenterology and Hepatology, Graduate School of Medicine, Mie University, Mie, Japan.
¶Current affiliation: Department of Laboratory Medicine, Clinical Research Center, Karolinska University Hospital, Huddinge, Sweden.

orientation of the passenger and guide sequences within the hairpin molecule has a profound impact on the RNAi-trigger's activity profile. Right-handed hairpin (RHP) loop RNAs, containing a 5′-passenger-loop-guide-3′ structure, generally induce stronger RNAi responses with the presence of a double-stranded stem length exceeding 19 base pairs (bp), a large loop, and a 3′ 2 nucleotide overhang as this structure facilitates crucial Dicer processing (Fig. 1A and Supplementary Fig. S1; Supplementary Data are available online at www.liebertpub.com/nat) [9–15]. In contrast, left-handed hairpin (LHP) loop RNAs, with a 5′-guide-loop-passenger-3′ structure (Fig. 1A and Supplementary Fig. S1), have been found to maintain RNAi potency independent of loop size and 3′ structure [9,13,14,16,17]. The difference in structural tolerance between RHPs and LHPs reflects alternative mechanisms of entry into the RNAi pathway. LHPs contain an exposed 5′ guide strand end that can bind readily to the Ago2 MID domain, whereas RHPs do not and therefore require specific ribonuclease processing of the loop to obtain a free 5′ guide strand end before Ago loading. Thus, the structural properties of functional small LHPs place them in a distinct class of RNAi-inducing molecules from RHPs.

Few studies have investigated the LHP class of RNAi triggers and none had examined fully 2′-modified LHPs, and so, to investigate the mechanistic processing of LHP-induced RNAi responses, we synthesized a series of LHPs targeting GFP, Luciferase, and Plk1 with deleted guide and passenger strand nucleotides proximal to a shortened intervening loop. We find that LHPs can be reduced in length from 51mers to minimal-length 32mers and still induce robust, specific RNAi responses. Not surprisingly, LHPs require greater than 13 nucleotides of complementary targeting sequence on the guide strand for induction of RNAi responses. Finally, we find that LHPs are processed in a Dicer-independent manner that requires Ago2 cleavage of the accompanying passenger strand, resulting in an extended 3′-end of the loaded guide strand that is well tolerated by Ago2. Together, these observations define the LHP structural requirements and determine the mechanism of LHP RNA processing.

Materials and Methods

Synthesis and purification of oligonucleotides

Oligonucleotides were synthesized on a BioAutomation Mermade-6 oligonucleotide synthesizer (Bioautomation, Plano, TX). Commercially available phosphoramidites were coupled as per manufacturer's recommendation (R.I. Chemicals, Orange, CA; Glen Research, Sterling, VA). Standard Q-T columns (Glen Research) were used for controlled pore glass. All oligonucleotides were purified by reverse phase HPLC with an Agilent 1200 Series Analytical HPLC (Agilent, Santa Clara, CA) on an Agilent Eclipse-XDB C18 column with linear acetonitrile gradients. Oligonucleotides were analyzed by MALDI-TOF mass spectrometry using an Applied Biosystems-DE-Pro MALDI-TOF mass spectrometer (Applied Biosystems, Foster City, CA), and gel electrophoresis using 15% acrylamide/7 M urea denaturing gels stained with methylene blue for single-stranded RNA or 15% acrylamide nondenaturing gels stained with ethidium bromide for double-stranded RNA. GFP1 siRNA: guide 5′-CUGGGUGCUCAGGUAGUGGUU-3′, passenger 5′-CCACTACCTGAGCACCCAGUU-3′. GFP2 siRNA: guide 5′-UCCUUGAAGAAGAUGGUGCUU-3′, passenger 5′-GCACCAUCUUCUUCAAGGAUU-3′. GFP6 siRNA: guide 5′-UCGGAUCUUGAAGUUCACCUU, passenger 5′-GGUGAACUUCAAGAUCCGAUU-3′. Firefly luciferase siRNA based on Pr004661.1: guide 5′-UCUUUAUGAGGAUCUCUCUUU-3′, passenger 5′-AGAGAGAUCCUCAUAAAGAUU-3′. PLK1 siRNA: guide 5′-UCUGUCUGAAGCAUCUUCUUU-3′, passenger 5′-AGAAGAUGCUUCAGACAGAUU-3′.

Cell culture, transfection, and knockdown assays

Human H1299 lung adenocarcinoma cells containing an integrated, constitutively expressed destabilized GFP (dGFP) reporter gene (~2 h half-life) or firefly Luciferase (Luc) reporter gene GL3 were cultured in DMEM (Invitrogen) supplemented with 5% fetal bovine serum (FBS) (SOURCE), 100 U/mL penicillin, and 100 U/mL streptomycin (Invitrogen). Cells were plated in 24-well plates at 40,000 cells/well for transfection of siRNA and LHP. Before treatment, cells were washed twice with serum-free DMEM. Transfection mixtures were prepared in 200 μL serum-free DMEM with 2 mL Lipofectamine 2000 (Invitrogen) and left at room temperature for 5 min before treatment. Transfection mixtures were added to cells and incubated for 6–8 h at 37°C before removal and the addition of DMEM with 5% FBS. For H1299-dGFP, cells were trypsinized for fluorescence analysis by FACS on an LSRII flow cytometer (BD Biosciences). For H1299-Luc, cells were washed twice with HBSS and incubated with 150 mg/mL luciferin (Gold Biotechnology) for luminescence analysis on an IVIS Spectrum (Caliper Life Sciences) imaging system. After imaging, cells were trypsinized and counted using an LSRII flow cytometer. Luciferase signals were normalized for viable cell count.

Human U2OS osteosarcoma cells were cultured in DMEM supplemented with 10% FBS, 100 U/mL penicillin, and 100 U/mL streptomycin. 300,000 U2OS cells were reverse transfected with 50 nM hairpin and 1 μL RNAiMAX in a six-well plate for 12 h. Cells were washed and split in three wells and analyzed 48 h posttransfection for DNA content by propidium iodide staining using FACS analysis and PLK-1 expression by quantitative PCR (qPCR) and western blot. Western blot was performed using mouse anti-PLK1 (Clone 3F8, sc-53751; SantaCruz) 1:1,000 and mouse anti-tubulin 1:1,000 (GTU-88; Sigma) followed by goat anti-mouse Ig-g-HRP 1:2,000 (SC-2005; Santa Cruz).

For qPCR with H1299-dGFP and U2OS cells, RNA was isolated with TRIzol (Invitrogen). The aqueous phase was mixed with equal volume of 70% ethanol and prepared on RNeasy columns (Qiagen). Real-time PCR was performed with 100 ng of total RNA using the TaqMan RNA-to-Ct 1 step kit and TaqMan predesigned probe and primer sets for GFP (probe: 5′-FAM-CCAGTCCGCCCTGAGCAAAG ACC-3′; forward primer: 5′-CTGCTGCCCGACAACCAC-3′; reverse primer: 5′-TCACGAACTCCAGCAGGAC-3′), PLK (HS00153444_m1) and GAPDH (4333764F) (Applied Biosystems).

Use of all human materials was under the auspices of a UCSD E&HS-approved protocol.

Preparation, transfection, and Argonaute 2 Co-IP of ^{32}P-labeled oligonucleotides

Four hundred picomols of oligonucleotide was 5′ labeled with 2.5 U T4 polynucleotide kinase (NEB) and 200 μCi

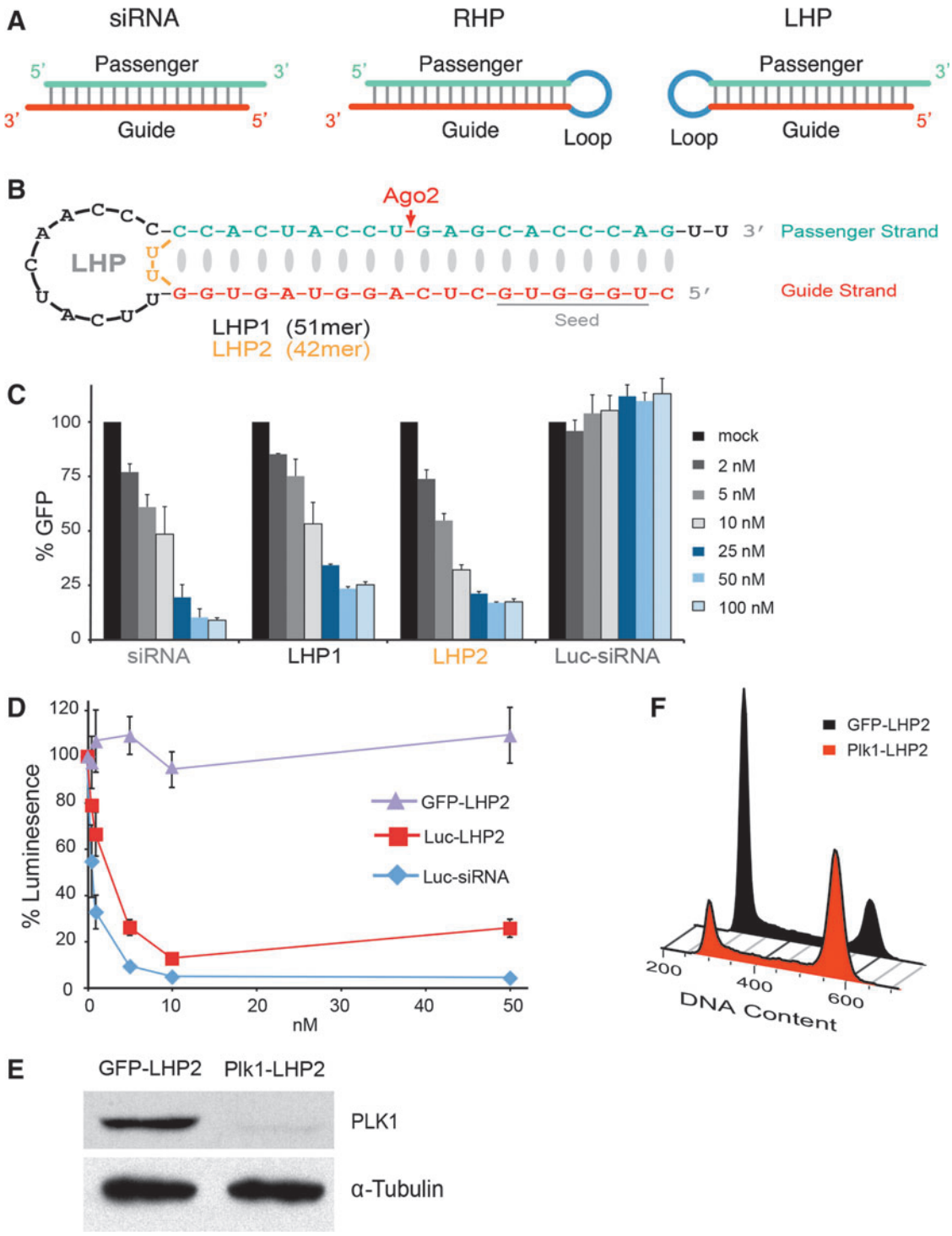

FIG. 1. Small 2′-F/OMe LHPs are functional for multiple target genes. **(A)** Diagrammatic representation of siRNA, RHP, and LHP structures. **(B)** LHP1 (*black*) and LHP2 (*gold*) structures of GFP1 targeting sequence. *Red arrow* indicates expected position of Ago2 passenger sequence cleavage. **(C)** Flow cytometry analysis of H1299-dGFP cells transfected with a dose curve of fully 2′-F/OMe-modified GFP1 siRNA, GFP1 LHP1, GFP1 LHP2, or control Luc siRNA. Cells were analyzed 48 h after transfection. **(D)** Luciferase activity of H1299-Luc cells 48 h after transfection with a dose curve of luciferase-targeted LHP2 or siRNA or control GFP LHP2. **(E)** Immunoblot analysis of U2OS osteosarcoma cells transfected with Plk1-targeted LHP2 or control GFP LHP2. **(F)** Flow cytometry analysis of U2OS osteosarcoma cells transfected with Plk1-targeted LHP2 or control GFP LHP2. Cells were stained with propidium iodide to measure DNA content. LHP, left-handed hairpin; RHP, right-handed hairpin.

^{32}P-ATP (6,000 Ci/mmol) in a 50 μL volume for 20 min. The reaction was inactivated for 20 min at 65°C and free ^{32}P-ATP was removed from the reaction mixture using G-25 spin columns (GE Healthcare). Marker labeling was performed in a 5% scale. Labeled LHP was diluted to a volume of 250 μL in Opti-MEMI and mixed with 250 μL Opti-MEM I containing 15 μL Lipofectamine 2000. After a 20-min incubation, the mixture was added to 2.4×10^6 H1299-dGFP cells in 8 mL DMEM containing 5% FBS and seeded in a 10-cm tissue culture dish. Cells were transfected for 12 h and washed with phosphate-buffered saline (PBS) before medium replacement.

Cells were washed with ice-cold PBS at 36 h posttransfection and lysed in 1 mL ice-cold lysis buffer [20 mM Tris-Hcl (pH 7.9), 250 mM NaCl, 0.5% Triton X-100, 0.1% DEPC, 0.5% protease inhibitor cocktail, and 1% phosphatase inhibitor cocktail II (Sigma)] for 10 min on ice. Lysates were cleared at 16,000*g* for 10 min at 4°C. Nine hundred microliters of cleared lysate was incubated with 100 μL of washed protein G-sepharose 4B slurry (Invitrogen) on a rotator at 4°C. After 2 h, beads were spun down and 850 μL of lysate was transferred to a tube containing 75 μL of washed protein G-sepharose 4B slurry preincubated for 2 h with 10 μL of anti-human Argonaute 2 antibody (4G8, 0.9 mg/mL; Wako Chemical USA, Richmond, VA) and incubated on a rotary shaker for 4 h. Beads were washed four times with ice-cold lysis buffer and eluted with 50 μL formamide/0.1% bromophenol at 95°C for 1 min. Eluates, markers, and input LHPs were counted on a scintillation counter and input counts were normalized to IP sample, heated at 95°C for 3 min, and snap cooled on dry ice/ethanol. Samples were thawed on ice and loaded on a 15% acrylamide/7 M urea/20% formamide PAGE. Gels were exposed to a phosphorImager screen at −20°C and analyzed on a phosphorImager Typhoon (Molecular dynamics). Tiff files were exported from ImageQuant and whole-image levels were adjusted in Adobe Photoshop without affecting gamma.

5′ Rapid amplification of cDNA ends

H1299-dGFP cells were transfected as described previously. RNA was isolated and purified with TRIzol and RNeasy columns 24 h posttransfection. Three micrograms of RNA was ligated to 0.25 μg GeneRacer RNA oligo (Invitrogen). Ligated RNA was reverse transcribed with superscript III and oligo dT(20). cDNA was amplified with the GeneRacer 5′ primer and GFP-specific primer (5′-CCGCT CTCCTGGGCACAAGAC-3′) using a step-down PCR protocol. PCR products were analyzed on a 1.2% agarose/TBE gel, and bands of predicted size were excised and purified with QIAquick gel extraction columns and reagents (Qiagen). Purified PCR products were sequenced directly.

Innate immune response and serum stability

Human peripheral blood mononuclear cells (PBMCs) were isolated from healthy donors as described before. 3×10^5 freshly isolated PBMCs were treated with 25, 100, 250, or 500 nM of 2′-OH or 2′-F/OMe 21-mer GFP siRNAs plus Lipofectamine and seeded onto a 96-well plate. Culture supernatants were collected at 24 h after addition and assayed for IFN-a (R&D systems). For serum stability, 50 pmol of 5′ IRdye-labeled siRNA guide strand was incubated in 50% human complement active serum (Innovative Research) at 37°C. At indicated time points, an aliquot was taken and diluted 10-fold in 7 M urea loading buffer. Samples were heated to 95°C for 1 min, flash frozen on dry ice, and stored at −80°C until analysis on a 15% acrylamide/7 M urea PAGE. Gels were analyzed on an Odyssey imager (LI-COR).

Results

Synthetic LHP RNAs are potent RNAi triggers

To understand LHP structural requirements for efficient induction of RNAi responses, we first synthesized a 51mer LHP targeting GFP, called LHP1, based on our previously published siRNA sequence to GFP, called GFP1 [16,17]. Starting from the 5′ end of the guide strand, LHP1 contains a 19 bp stem with an 11 nucleotide (nt) single-stranded loop, followed by 19 bp of complementary passenger strand and 3′ dinucleotide overhang (Fig. 1A and Supplementary Fig. S1). We also synthesized a similarly designed LHP, but with a stabilized 2 nt U-U loop [18–20], called LHP2 (42mer) (Fig. 1B). In addition, we synthesized a canonical 21mer GFP1-siRNA with 3′ dinucleotide overhangs and a control luciferase (Luc) targeted Luc-siRNA. To avoid activation of the innate immune system [7,21,22], all RNAi triggers were synthesized with 2′-F on all pyrimidines and 2′-OMe on all purines. 2′-F/OMe modifications are highly tolerated by the RNAi machinery and used extensively on therapeutic siRNAs in clinical trials [23–25].

To analyze for induction of RNAi responses, RNAi triggers were transfected in a dose-dependent manner into human H1299 lung adenocarcinoma cells constitutively expressing a destabilized GFP [16,17] and analyzed by flow cytometry and quantitative real time-PCR (Fig. 1C and Supplementary Fig. S2). GFP1-LHP1, which contains an 11 nt loop, induced a dose-dependent GFP RNAi response that was moderately less efficient than the parental GFP1-siRNA. However, GFP LHP2, which contains a constrained two nucleotide UU loop, induced GFP RNAi responses closer to the siRNA-induced RNAi response. As expected, control luciferase-targeted siRNA failed to induce an RNAi response at any of the tested concentrations (Fig. 1C). Similar results were obtained with two additional independent GFP sequences (GFP2 and GFP6) (Fig. 5). Together, these observations demonstrate that 42mer LHP2 RNAs are efficient RNAi triggers.

To confirm the functionality of 2′-F/OMe LHPs for multiple target genes, we designed and produced 2 nt loop LHP2s targeting the firefly Luciferase (Luc) reporter gene GL3 and the Polo-Like Kinase-1 (Plk1) endogenous proto-oncogene following the same design rules used for GFP LHPs. Transfection of Luc-LHP2 into H1299 cells constitutively expressing GL3 luciferase induced potent RNAi responses (Fig. 1D), similar in magnitude to those observed by GFP-LHP2. We next targeted Plk1 in U2OS cells where Plk1 depletion induces a phenotypic G2 phase cell cycle arrest [26,27]. At 48 h posttransfection, 2′-F/OMe Plk1-LHP2-treated cells displayed a strong reduction in Plk1 protein compared to control GFP1-LHP2 (Fig. 1E). The Plk1 knockdown was paralleled by induction of a G2/M phase cell cycle arrest (Fig. 1F). These results demonstrate that 2′-F/OMe-modified, minimal loop LHP molecules are efficient RNAi triggers for both reporter and endogenous genes.

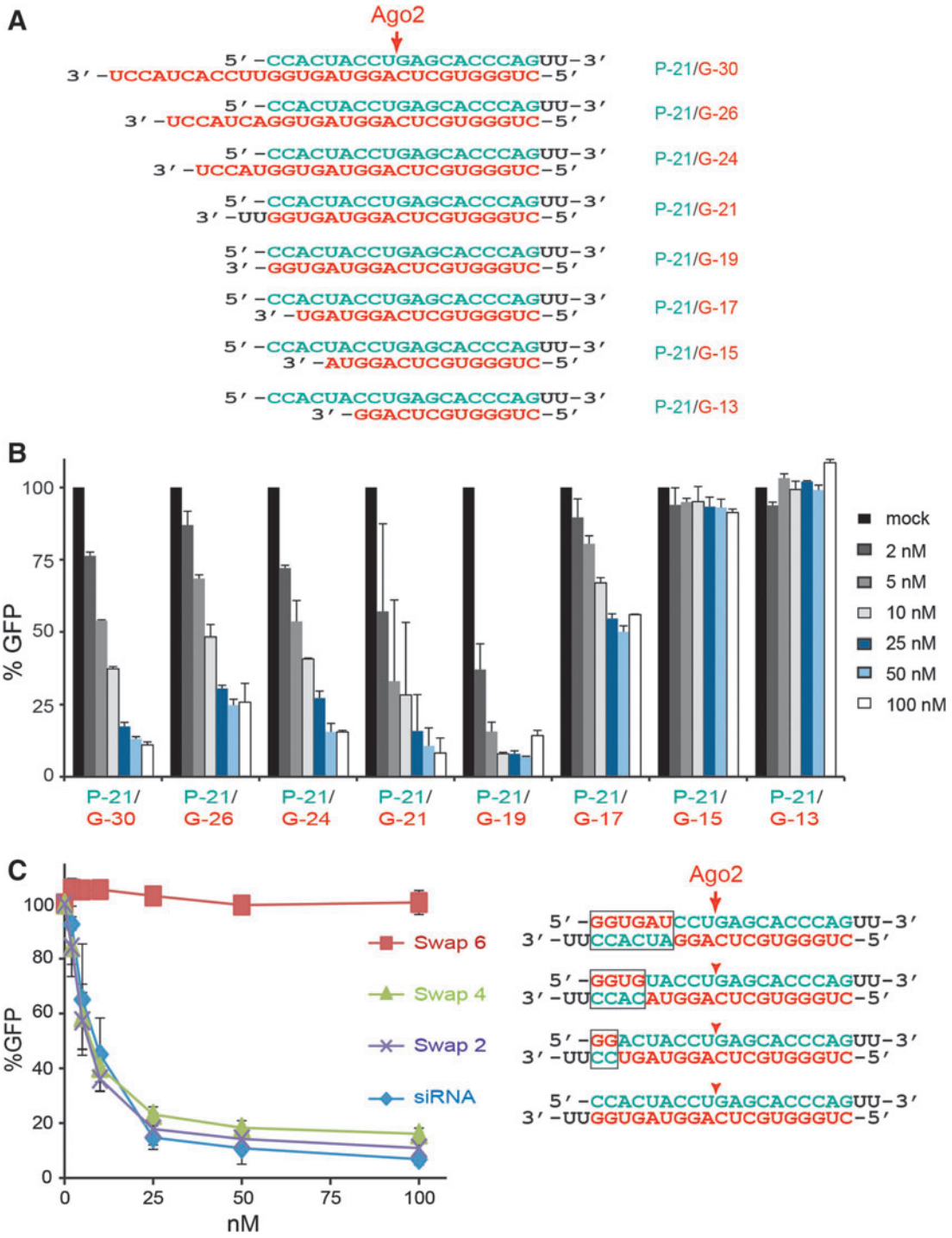

FIG. 2. Tolerance of RNAi machinery for structure and sequence alteration of RNAi triggers. **(A)** Structures of 2′-F/OMe GFP1 siRNAs studied with variable guide strand lengths annealed to 21 nt passenger strand. *Red arrow* indicates position of Ago2 passenger strand cleavage. **(B)** Flow cytometry analysis of H1299-dGFP cells 48 h after transfection with dose curves of GFP1 siRNAs containing variable length guide strands. **(C)** *Right panel*: structures of passenger/guide strand sequence exchanged GFP1 siRNAs. *Left panel*: flow cytometry analysis of H1299-dGFP cells 48 h after transfection with dose curves of sequence exchanged siRNAs.

Structural determinants of LHP

LHPs induce RNAi responses in cells independent of Dicer or single-stranded RNase processing [14]. However, due to the unique design of LHPs, Ago2 can clip the attached passenger strand, releasing a 12 nt fragment from the 3′ end, but retaining the 5′ half of the embedded passenger strand (Fig. 1B). The result is that Ago2 retains an elongated ''guide'' strand that contains the core guide strand attached to the loop and 5′ end of the cleaved passenger strand. For

example, a 42mer LHP2 (5′ 19 nucleotide guide, 2 nt loop, 19 nt passenger, and 3′-UU overhang) will be processed by Ago2 into a 30 nucleotide guide strand. To explore the tolerance of Ago2 for extended length guide strands, we annealed a 21mer GFP passenger strand (P-21) to GFP guide strands ranging from 13 to 30 nts with the 5′ end fixed and the increased length added to the 3′ end (Fig. 2A). The double-stranded siRNAs were transfected in H1299-GFP cells and assayed for GFP knockdown by FACS at 48 h (Fig. 2B). GFP guide strand oligonucleotides of 24, 26, and 30 nt all induced RNAi responses similar to those observed with the standard siRNA guide strand of 21 bases (Fig. 2B). Consistent with previous studies [28], reduction in guide strand length to 19 nt was well tolerated. However, further reduction to 17 nt on the guide strand resulted in a significant loss of RNAi activity (Fig. 2B). Further reduction to 15 and 13 nt guide strands was completely inactive. These results showed that having a long ''3′ tail'' on the guide strand does not interfere with induction of RNAi responses.

LHPs can induce RNAi responses with minimal-size hairpin structures (see LHP2, Fig. 1). However, the minimal size limitations of LHPs have not been thoroughly investigated. Reduction in LHP size can be achieved by shortening the passenger strand, guide strand, loop, and/or a combination of all three [14,19]. However, a negative consequence of shortening the guide strand sequence is loss of mRNA complementary targeting sequence. To investigate guide strand requirements for induction of RNAi responses, we swapped the complementary 5′ guide and 3′ passenger strand sequences of the GFP1 siRNA, which contains 19 bases

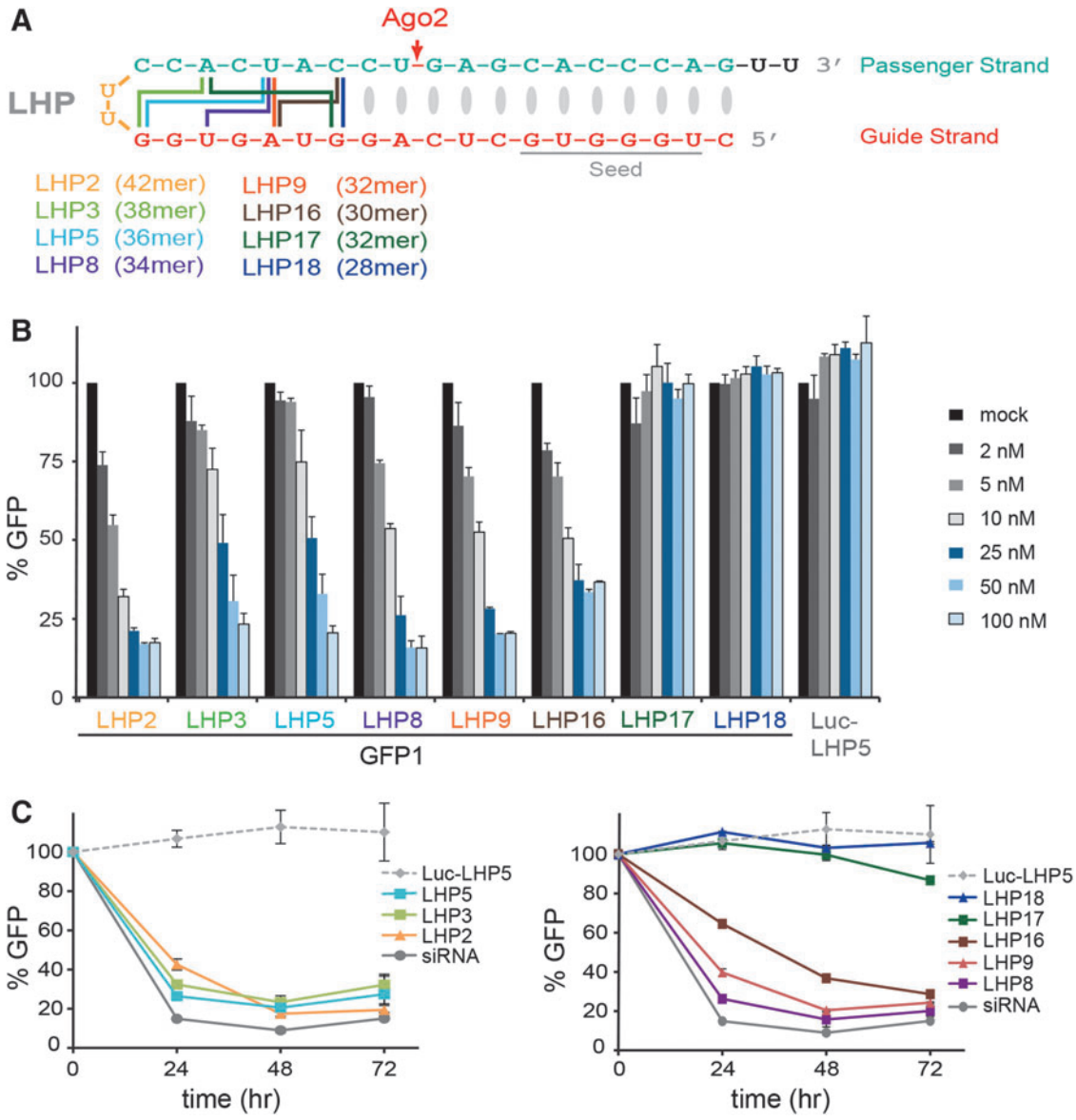

FIG. 3. Exploration of size reduction in LHPs with 3′-dinucleotide overhangs. **(A)** Structures of size-reduced 2′-F/OMe GFP1 LHPs containing a 3′-UU overhang. *Red arrow* indicates position of Ago2 passenger sequence cleavage. **(B)** Flow cytometry analysis of H1299-dGFP cells 48 h after transfection with dose curves of size-reduced GFP1 LHPs containing 3′-UU overhangs or control luciferase-targeted LHP5. **(C)** Kinetic analysis by flow cytometry of RNAi responses in H1299-dGFP cells transfected with 100 nM LHPs or siRNAs.

complementary to the GFP mRNA plus a 2 nt UU 3′ tail (21 nt total) (Fig. 2C). As a result, all siRNAs retained identical thermodynamic properties (Tm) for loading into Ago2 compared to the parental siRNA sequence [29]. siRNAs with guide strands containing 17 and 15 nt of mRNA complementary target sequence (but remained 21 nt long in total) induced a near-identical, RNAi dose/response curve as the 19 nt complementary base (21 nt total length) of the parental siRNA (Fig. 2C). However, the siRNA with only 13 matched bases of mRNA complementary sequence showed no RNAi activity. These observations established a lower limit to the guide strand sequence of 15 complementary bases in reducing the LHP overall size.

Minimal size limits of LHPs

Previous studies have shown highly functional LHP designs with 19 nt guide strands, 17, 18, or 19 nt passenger strands, and 2 nt UU loops [14,19]. To define the minimal necessary lengths of each strand, we synthesized a series of smaller LHPs with 3′-UU overhangs (Fig. 3A). LHP3 (38mer) contains a 19 nt guide strand linked directly to a 17 nt passenger strand (LHP3), which eliminated 4 nt from the LHP2 design. LHP3 efficiently knocked down dGFP expression with a low nanomolar EC_{50} and showed only a minimal change from LHP2 (Fig. 3B, C). Additional truncation of the passenger strand to 15 nt (LHP5, 36mer) also maintained high efficacy to induce a GFP RNAi response. We observed similarly potent RNAi activities using LHP8, a 34mer that contained 17 nt guide and 15 nt passenger strands. Surprisingly, further reduction to LHP9, a 32mer, with 15 nt guide and 15 nt passenger strands also showed similarly strong induction of RNAi responses. However, further reduction to LHP16, a 30mer with 15 nt guide and 13 nt passenger strands, resulted in measurably diminished RNAi responses (Fig. 3B, C). Consistent with our observations using independently synthesized guide strands (Fig. 2B), reduction of guide strand length to 13 nt

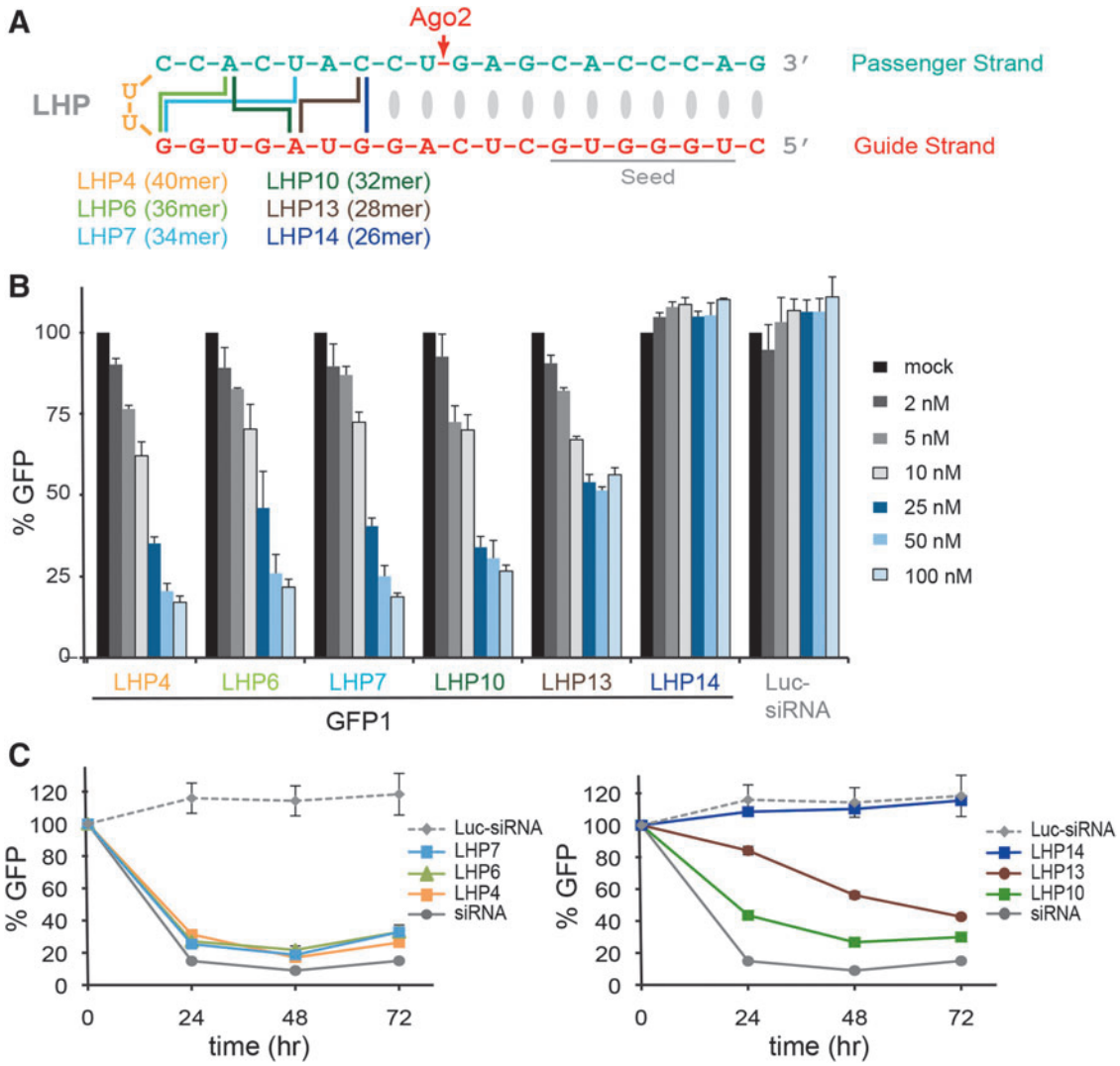

FIG. 4. Exploration of size reduction in blunt-ended LHPs. **(A)** Structures of size-reduced 2′-F/OMe GFP1 blunt-ended LHPs. *Red arrow* indicates position of Ago2 passenger sequence cleavage. **(B)** Flow cytometry analysis of H1299-dGFP cells 48 h after transfection with dose curves of size-reduced GFP1 blunt-ended LHPs or control luciferase-targeted siRNA. **(C)** Kinetic analysis by flow cytometry of RNAi responses in H1299-dGFP cells transfected with 100 nM LHPs or siRNAs.

with a 17 nt passenger strand (LHP17, 32mer) or a 13 nt passenger strand (LHP18, 28mer) completely abolished RNAi activity (Fig. 3B, C).

The LHPs discussed above (LHP2, 3, 5, 8, 9, 16, 17, 18) all have 3′-UU overhangs over the 5′ end of the guide strand; however, the 3′ overhang on siRNAs is required for optimal PAZ binding to the 3′ end of the guide strand (not the 5′ end of the guide in the LHP configuration) [21,23,24]. Consistent with this, a high-caliber clinical candidate siRNA (AT3) contains a blunt 5′ end of the guide strand with a two nt 3′ overhang [23]. Therefore, we generated and assayed a second set of LHPs that had removed the 3′-UU passenger strand overhang (Fig. 4A). Overall, blunt ended LHPs demonstrated similar RNAi activities (Fig. 4B, C) similar to their 3′-UU overhang counterparts (Fig. 3B, C). Potent RNAi responses were observed with LHP4 (40mer) (similar to LHP2) containing a 19 nt guide strand and 19 nt passenger strand, LHP6 (36mer) (similar to LHP3) containing a 19 nt guide strand and 17 nt passenger strand, LHP7 (34mer) (similar to LHP5) containing a 19 nt guide strand and 15 nt passenger strand, and LHP10 (32mer) containing a 15 nt guide strand and 17 nt passenger strand (Fig. 4B, C). Similar to LHP 16, activity started to drop off for LHP13 (28mer) with a 15 nt guide strand and 13 nt passenger strand, and was completely lost with LHP14 (26mer) (similar to LHP18) containing a 13 nt guide strand and 13 nt passenger strand. Together, these results established a minimal size for high-caliber LHP induction of RNAi responses of 32 nt (LHP9: 15 nt guide, 15 nt passenger).

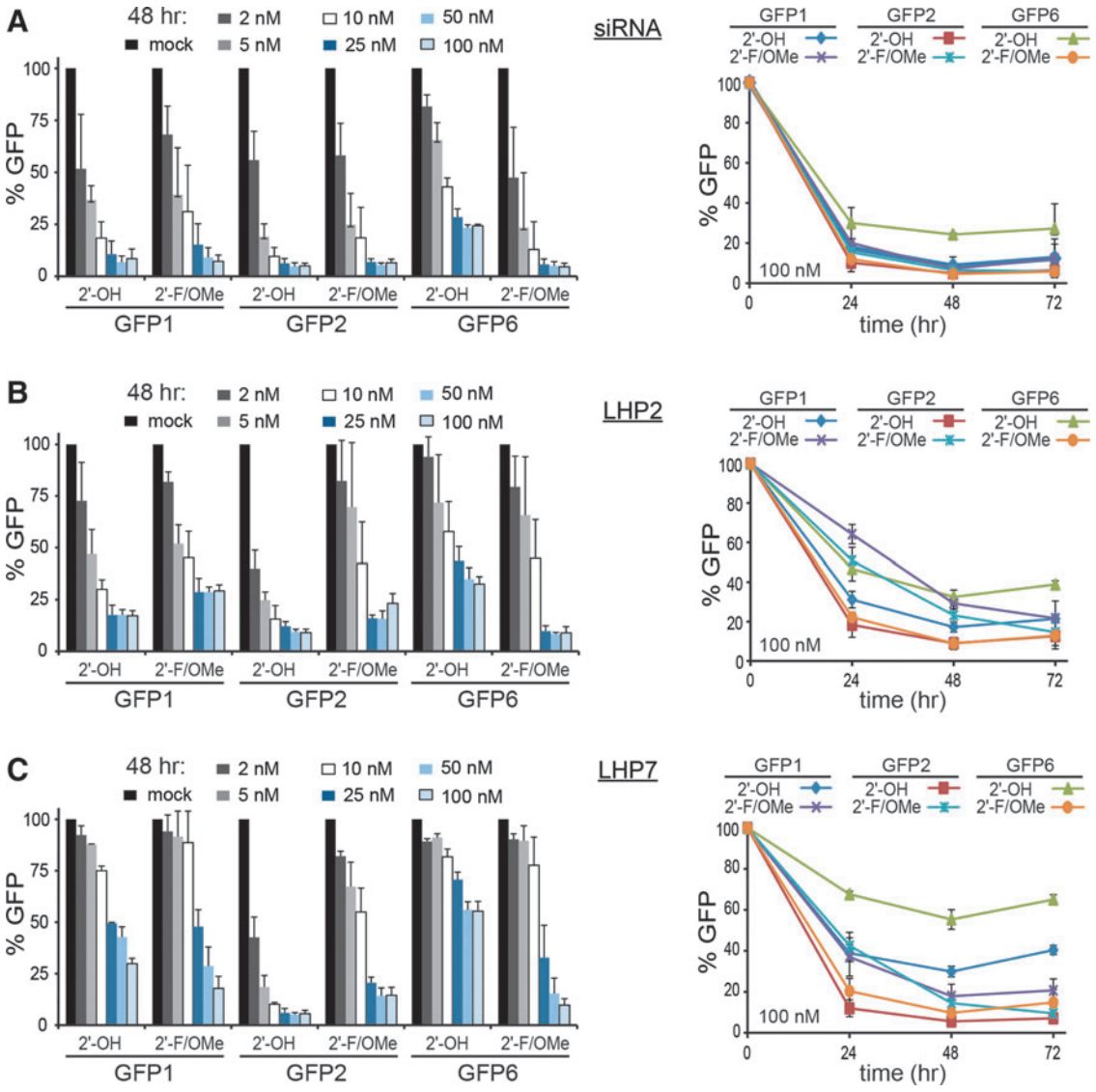

FIG. 5. Comparison of three distinct GFP targeting sequences using siRNA, LHP2, and LHP7 structures containing 2′-OH or 2′-F/OMe groups. **(A)** *Left panel*: flow cytometry analysis of H1299-dGFP cells 48 h after transfection with dose curves of GFP-targeted siRNA containing 2′-OH or 2′-F/OMe groups. GFP1, GFP2, and GFP6 are three discrete siRNA sequences all targeting GFP. *Right panel*: kinetic analysis by flow cytometry of RNAi responses in H1299-dGFP cells transfected with 100 nM siRNA. **(B)** Forty-eight-hour dose curve and 3-day kinetic analysis of cells transfected with LHP2 molecules. **(C)** Forty-eight-hour dose curve and 3-day kinetic analysis of cells transfected with LHP7 molecules.

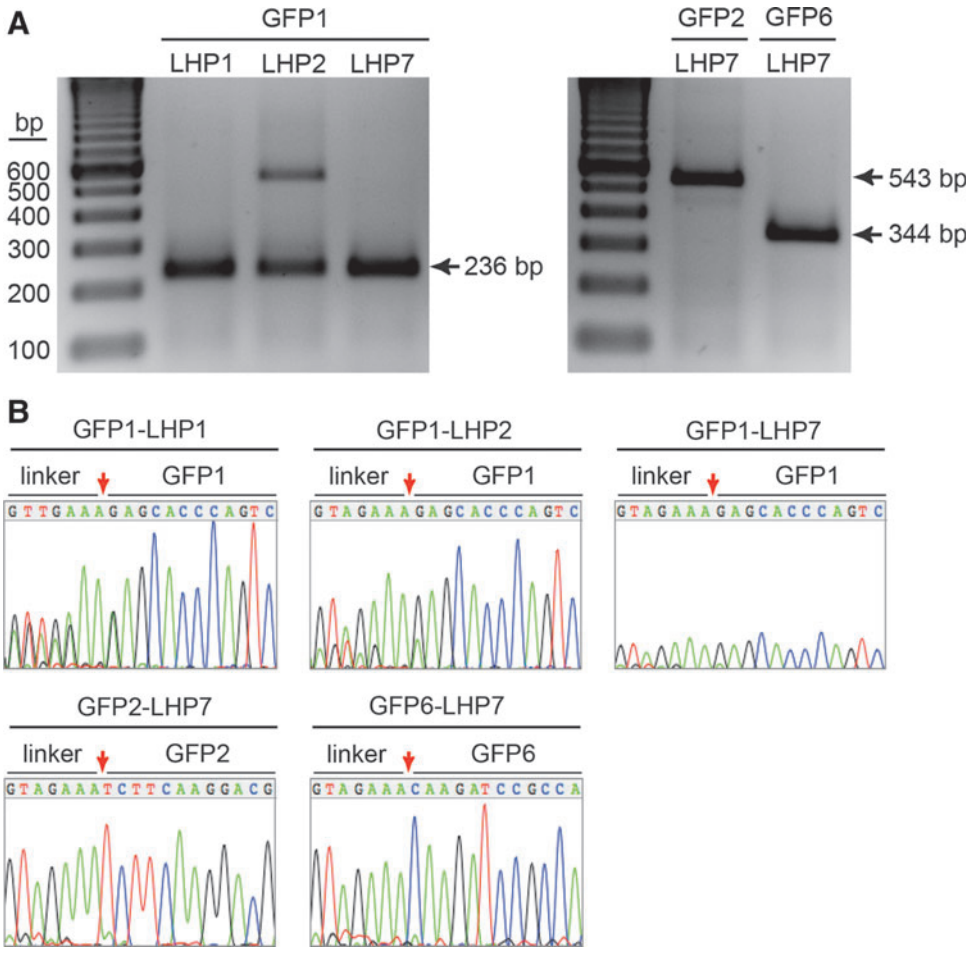

FIG. 6. 5′-RACE analysis of GFP mRNA from H1299-dGFP cells transfected with 2′-F/OMe LHPs. **(A)** 5′ RACE analysis of H1299-dGFP cells transfected with GFP-targeted LHPs. PCR amplification products of anticipated size for GFP1 (236 bp), GFP2 (534 bp), and GFP6 (344 bp) targeted LHPs. **(B)** Results of direct sequencing analysis of gel-purified 5′ RACE products. *Red arrow* indicates correct Ago2 cleavage site. PCR, polymerase chain reaction; RACE, rapid amplification of cDNA ends.

Multiple GFP targeting sequences function in the LHP configuration

We next studied the ability of three independent GFP RNAi sequences to function in two different LHP configurations. GFP1, GFP2, and GFP6 RNAi trigger sequences were synthesized as siRNAs (42mer total, two 21mers with 3′-UU overhangs on both ends), LHP2 (42mer, 19 nt guide, 19 nt passenger with a 3′-UU overhang), and LHP7 (34mer, 19 nt guide, 15 nt passenger, no 3′ overhang). Transfection of each siRNA construct into H1299-GFP cells resulted in potent and sustained RNAi responses by all three siRNA GFP target sequences when composed of either 2′-OH or 2′-F/OMe oligonucleotides (Fig. 5A). We note that the 2′-modified GFP6 siRNA was more potent than the corresponding 2′-hydroxyl siRNA. Although each LHP2 version of the GFP RNAi triggers induced strong RNAi responses, for the most part, these LHP2 RNAi responses demonstrated modestly diminished potency compared to their siRNA RNAi trigger counterparts (Fig. 5B). LHP size reduction to the LHP7 structure resulted in lowered efficacy for most sequences (Fig. 5C), with only the GFP2 molecule inducing knockdown efficacy equivalent to its LHP2 counterpart.

A hallmark of RNAi responses is the specific cleavage of target mRNA opposite nucleotides 10–11 of the guide strand [24]. We confirmed RNAi as the mechanism of GFP knockdown for LHPs by performing 5′ rapid amplification of cDNA ends (RACE) analysis (Fig. 6). LHP1, LHP2, and LHP7 molecules targeting the GFP1 sequence all generated 5′ RACE PCR products of the predicted size (236 bp) (Fig. 6A). LHP7 molecules targeting the GFP2 and GFP6 sequences also yielded expected size PCR products (543 and 344 bp, respectively) (Fig. 6A). Direct sequencing of gel-purified PCR products confirmed the predicted cleavage

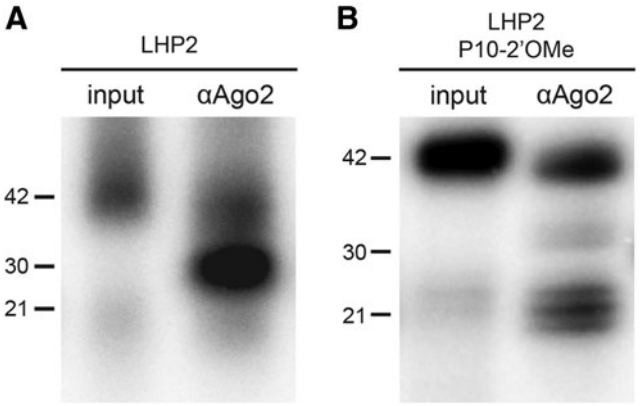

FIG. 7. Ago2 Co-IP of ^{32}P-labeled 2′-F/OMe LHPs. Anti-Ago2 coimmunoprecipitation from cells transfected with **(A)** ^{32}P-labeled GFP1-LHP2 with a cleavable 2′-F at the passenger strand cleavage site, and **(B)** ^{32}P-labeled GFP1-LHP2 with a noncleavable 2′-OMe at the passenger strand cleavage site. Input is ^{32}P-labeled 42mer LHP2. Molecular weight markers are ^{32}P-labeled 42mer, 30mer, and 21mer as indicated on *left* side.

site for each of the LHPs (Figs. 3A, 4A, and 6B). Interestingly, both GFP1-LHP1 and LHP2 appear to induce RISC-mediated mRNA cleavage on a fraction of transcripts opposite nucleotides 11–12 of the guide sequence (Fig. 6B). This apparent slight flexibility in the active site of Ago2 could be the consequence of large guide strands that result from Ago2 processing of LHPs (LHP1: 39 nt, LHP2: 30 nt). Indeed, the observed effect correlated positively with predicted guide strand size of the LHPs as RISC loaded with LHP7 molecules (shorter guide strand following Ago2 passenger cleavage) targeting all three GFP sequences demonstrated perfect specificity for the classic mRNA cleavage site (Fig. 6B).

LHPs are activated by Ago2 processing

LHPs are thought to be processed in a Dicer- and RNase-independent manner [14]. To investigate the mechanism of LHP-induced RNAi responses, we 5′ end labeled LHPs with ^{32}P, transfected them into cells, then immunoprecipitated endogenous Ago2, and assayed for the size of the associated to ^{32}P LHP fragments. If LHP-mediated RNAi responses are independent of Dicer or single-stranded RNase cleavage of the loop, mature RISC will contain a long guide strand (guide strand plus loop and 5′ fragment of passenger strand). Coimmunoprecipitation of 5′ ^{32}P-labeled LHP2 with anti-Ago2 resulted in identification of a ^{32}P oligonucleotide with size equivalent to the 30 nt marker (Fig. 7A). This 30mer is the exact length that would be expected from LHP2 passenger cleavage by Ago2 (19 nt guide, 2 nt loop, plus 9 nt passenger fragment) (Fig. 1A). While a 2′-F is well tolerated at the Ago2 passenger strand cleavage site, insertion of a 2′-OMe strongly inhibits Ago2 cleavage [14]. Transfection and anti-Ago2 immunoprecipitation of ^{32}P-labeled LHP2 with a 2′-OMe at the passenger strand cleavage site resulted in identification of the 42 nt parental LHP, plus several small fragments at 20, 21, and 22 nt that were not seen with the parental LHP2 (some small) (Fig. 7B). The 2′-OMe LHP2 also failed to induce a GFP RNAi response (Supplementary Fig. S3). These observations are consistent with the Ago2-guide strand crystal structure showing that nucleotides 15 to 19 are unstructured and looped out [30], suggesting a potential mechanism to accommodate the longer guide strands resulting from LHP Ago2 processing.

Discussion

Induction of RNAi responses requires TRBP loading of a double-stranded A-form RNAi trigger that is processed on Ago to remove the passenger strand resulting in a nucleotide-exposed, guide strand [7,24,25]. The vast majority of work on exogenous, nonexpressed RNAi triggers has focused on siRNA-like structures based on the Tuschl laboratory's prototypical two 21 nt oligonucleotide strands with 3′ overhangs [3]. Derivatives of this include blunt end on either or both siRNA ends, siRNAs of longer and shorter strands, and Dicer substrates that contain an extended region beyond the mature 5′ end of the guide strand category [24]. Excluding a few rare examples, such as miR-451, the vast majority of endogenously expressed (transcribed) miRNAs are in a RHP stem-loop structure with a loop that is processed in the cytoplasm by Dicer, followed by TRBP loading into Ago [12,31–33]. However, there are no currently known examples of endogenous LHP miRNAs configured with a very short loop. Consequently, short looped LHPs represent a novel synthetic RNAi trigger.

Here comparing three different LHP RNAi triggers to GFP, our structure/activity relationship analyses defined the minimal size of the LHP and the guide strand length required for induction of robust RNAi responses. Prior studies on LHPs laid down the ground work for characterizing these unique RNAi triggers [14,18,19]. Because LHPs are not processed by Dicer [14], to activate an LHP, the intact full-length LHP must first be loaded by TRBP into Ago2 and then have its passenger strand cleaved by Ago2. This results in an extended 3′ guide strand ''tail'' that at the 3′ end is composed of the 5′ end fragment of the passenger strand (Fig. 8). Given the mechanism of LHP activation and that the passenger strand is covalently attached to the guide strand, we speculate that LHPs loaded into noncatalytic Ago1, 3, 4 would remain double stranded in a nonfunctional configuration versus catalytically active Ago2. Importantly, because miRNAs have guide strands between 19 and 27 nt long, Ago has been evolutionary designed to accommodate extended 3′ tails on guide strands [30,34]. Consequently, the critical guide strand seed and cleavage site remain in the same structural regions of Ago2 regardless of guide strand length [34]. To

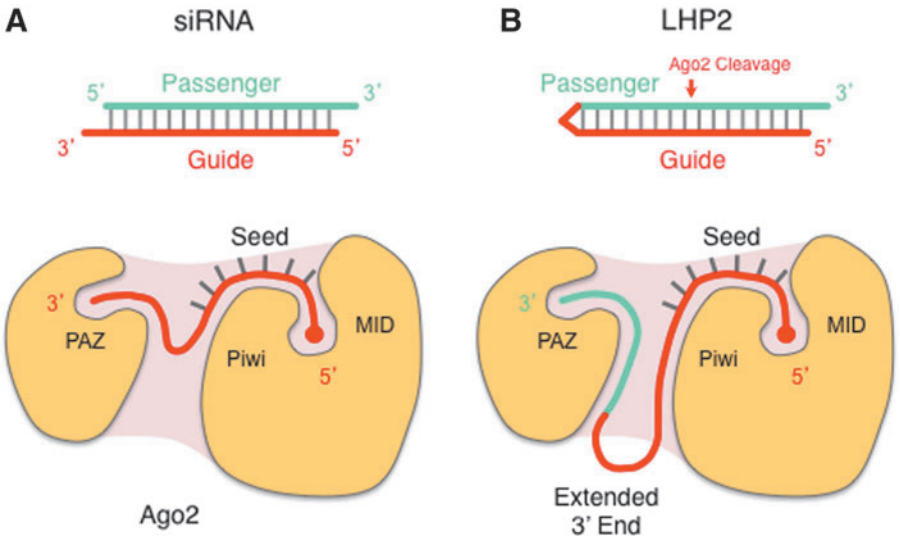

FIG. 8. Diagram of loaded guide strand from siRNA **(A)** vs. loading of extended guide strand with 5′ end of passenger strand in LHP2 **(B)**.

accommodate the varying length guide strands, the central region of the 3′ tail is looped out and unstructured in the Ago2 structure, followed by the last two nt of the 3′ end loaded into the PAZ domain [30]. Similar to longer miRNAs, we speculate that the extended 3′ tails of cleaved LHPs are looped out on Ago2 (Fig. 8).

Unlike siRNAs, LHP molecules are composed of a single oligonucleotide and are therefore generated from a single-column synthesis. In addition, use of minimal length LHPs (32 nt) versus siRNAs (42 total nt) can lower overall production costs. Due to their structure, LHPs also eliminate unintended off-target silencing from passenger strand loading into Ago2, as can occur with siRNA. LHPs with 2 nt 3′ overhangs consistently performed better in our hands than did blunt-ended LHPs (Figs. 3 and 4). Because, 5′ guide strand blunt-ended siRNAs are the preferred RNAi trigger in clinical trials [23], we do not currently have a mechanistic basis for this observation. Importantly, Ago2 cleavage of the LHP is a critical requirement as blocking this cleavage with a 2′-OMe on the passenger cleavage site completely killed LHP processing and the RNAi response (Fig. 7).

Beyond the scope of the work presented here, we ask the question: What do single-strand LHPs do that is better/different than standard, double-stranded siRNAs at this stage in the clinical development of RNAi therapeutics? The answer is that while double-stranded siRNAs work exceptionally well for GalNAc-mediated delivery to liver hepatocytes [7,23–25], this is a first-pass targeting strategy that relies heavily on the overabundance of the hepatocyte asialoglycoprotein receptor (ASGPR) ($\sim 10^6$ receptors/cell) to sequester the low blood concentration of GalNAc-siRNAs that slowly drip into the blood stream from their subcutaneous depot before they come in contact with, and are filtered out by, the kidneys. Indeed, due to the saturation of ASGPR, the majority of an i.v. bolus injection of GalNAc-siRNAs ends up being filtered out by the kidney, resulting in an extremely poor RNAi response [17]. With the exception perhaps of the transferrin receptor (CD71), there are no other examples of ligand/receptor pairs that have this extremely high level of receptors ($\sim 10^6$) and that are turned over extremely rapidly (~ 15 min) [7]. Most receptors to be targeted are in the 10^4 to 10^5 range and turn over every 90 min, resulting in a dramatically smaller amount of RNAi trigger entering the endosome on an hourly basis. Consequently, to obtain as many shots-on-goal as possible, extrahepatic delivery of RNAi triggers will need to remain stable and intact in the blood stream for as long as possible. Beyond the size reduction and single-stranded synthetic simplicity, LHPs offer an inherent stabilization design that exposes only a single end to exonucleases (vs. two for siRNAs). In summary, we believe that development of robust extrahepatic RNAi delivery systems will require alternative RNAi trigger designs versus the double-stranded siRNA approach used for the liver. LHPs represent a unique class of RNAi triggers that may present advantages as the field begins to move beyond GalNAc delivery to the liver.

Author Disclosure Statement

S.F.D is a member of the board of directors of Solstice Biologic. S.F.D is a cofounder, and B.R.M is a cofounder and employee of Solstice Biologics, a biotech company developing RNAi therapeutics. All other authors have no conflicts of interest to declare.

References

1. Fire A, S Xu, MK Montgomery, SA Kostas, SE Driver and CC Mello. (1998). Potent and specific genetic interference by double-stranded RNA in *Caenorhabditis elegans*. Nature 391:806–811.
2. Ender C and G Meister. (2010). Argonaute proteins at a glance. J Cell Sci 123:1819–1823.
3. Elbashir SM, J Harborth, W Lendeckel, A Yalcin, K Weber and T Tuschl. (2001). Duplexes of 21-nucleotide RNAs mediate RNA interference in cultured mammalian cells. Nature 411:494–498.
4. Hahn WC and RA Weinberg. (2002). Modelling the molecular circuitry of cancer. Nat Rev Cancer 2:331–341.
5. Wittrup A and J Lieberman. (2015). Knocking down disease: a progress report on siRNA therapeutics. Nat Rev Genet 16:543–552.
6. Kacsinta AD and SF Dowdy. (2016). Current views on inducing synthetic lethal RNAi responses in the treatment of cancer. Expert Opin Biol Ther 16:161–172.
7. Dowdy SF. (2017). Overcoming cellular barriers for RNA therapeutics. Nat Biotech 35:222–229.
8. Kim D-H, MA Behlke, SD Rose, M-S Chang, S Choi and JJ Rossi. (2005). Synthetic dsRNA Dicer substrates enhance RNAi potency and efficacy. Nat Biotechnol 23:222–226.
9. Harborth J, SM Elbashir, K Vandenburgh, H Manninga, SA Scaringe, K Weber and T Tuschl. (2003). Sequence, chemical, and structural variation of small interfering RNAs and short hairpin RNAs and the effect on mammalian gene silencing. Antisense Nucleic Acid Drug Dev 13:83–105.
10. Siolas D, C Lerner, J Burchard, W Ge, PS Linsley, PJ Paddison, GJ Hannon and MA Cleary. (2005). Synthetic shRNAs as potent RNAi triggers. Nat Biotechnol 23:227–231.
11. Vlassov AV, B Korba, K Farrar, S Mukerjee, AA Seyhan, H Ilves, RL Kaspar, D Leake, SA Kazakov and BH Johnston. (2007). shRNAs targeting hepatitis C: effects of sequence and structural features, and comparision with siRNA. Oligonucleotides 17:223–236.
12. Rao DD, JS Vorhies, N Senzer and J Nemunaitis. (2009). siRNA vs. shRNA: similarities and differences. Adv Drug Deliv Rev 61:746–759.
13. McManus MT, CP Petersen, BB Haines, J Chen and PA Sharp. (2002). Gene silencing using micro-RNA designed hairpins. RNA 8:842–850.
14. Dallas A, H Ilves, Q Ge, P Kumar, J Shorenstein, SA Kazakov, TL Cuellar, MT McManus, MA Behlke and BH Johnston. (2012). Right- and left-loop short shRNAs have distinct and unusual mechanisms of gene silencing. Nucleic Acids Res 40:9255–9271.
15. Liu YP, NCT Schopman and B Berkhout. (2013). Dicer-independent processing of short hairpin RNAs. Nucleic Acids Res 41:3723–3733.
16. Eguchi A, BR Meade, Y-C Chang, CT Fredrickson, K Willert, N Puri and SF Dowdy. (2009). Efficient siRNA delivery into primary cells by a peptide transduction domain-dsRNA binding domain fusion protein. Nat Biotechnol 27:567–571.
17. Meade BR, K Gogoi, AS Hamil, C Palm-Apergi, A van den Berg, JC Hagopian, AD Springer, A Eguchi, AD Kacsinta, *et al.* (2014). Efficient delivery of RNAi prodrugs containing reversible charge-neutralizing phosphotriester backbone modifications. Nat Biotechnol 32:1256–1261.
18. Ge Q, A Dallas, H Ilves, J Shorenstein, MA Behlke and BH Johnston. (2010). Effects of chemical modification on the

potency, serum stability, and immunostimulatory properties of short shRNAs. RNA 16:118–130.
19. Ge Q, H Ilves, A Dallas, P Kumar, J Shorenstein, SA Kazakov and BH Johnston. (2010). Minimal-length short hairpin RNAs: the relationship of structure and RNAi activity. RNA 16:106–117.
20. Woese CR, S Winker and RR Gutell. (1990). Architecture of ribosomal RNA: constraints on the sequence of ''tetraloops.'' Proc Natl Acad Sci U S A 87:8467–8471.
21. Behlke MA. (2008). Chemical modification of siRNAs for in vivo use. Oligonucleotides 18:305–319.
22. Judge A and I MacLachlan. (2008). Overcoming the innate immune response to small interfering RNA. Hum Gene Ther 19:111–124.
23. Sehgal A, S Barros, L Ivanciu, B Cooley, J Qin, T Racie, J Hettinger, M Carioto, Y Jiang, *et al.* (2015). An RNAi therapeutic targeting antithrombin to rebalance the coagulation system and promote hemostasis in hemophilia. Nat Med 21:492–497.
24. Juliano RL. (2016). The delivery of therapeutic oligonucleotides. Nucleic Acids Res 347:6518–6548.
25. Khvorova A and JK Watts. (2017). The chemical evolution of oligonucleotide therapies of clinical utility. Nat Biotechnol 35:238–248.
26. Liu X and RL Erikson. (2003). Polo-like kinase (Plk)1 depletion induces apoptosis in cancer cells. Proc Natl Acad Sci U S A 100:5789–5794.
27. Kolosenko I, E Edsbäcker, A-C Björklund, AS Hamil, O Goroshchuk, D Grandér, SF Dowdy and C Palm-Apergi. (2017). RNAi prodrugs targeting Plk1 induce specific gene silencing in primary cells from pediatric T-acute lymphoblastic leukemia patients. J Control Release 261:199–206.
28. Chu C-Y and TM Rana. (2008). Potent RNAi by short RNA triggers. RNA 14:1714–1719.
29. Preall JB, Z He, JM Gorra and EJ Sontheimer. (2006). Short interfering RNA strand selection is independent of dsRNA processing polarity during RNAi in Drosophila. Curr Biol 16:530–535.
30. Schirle NT and IJ MacRae. (2012). The crystal structure of human Argonaute2. Science 336:1037–1040.
31. Yang J-S, T Maurin, N Robine, KD Rasmussen, KL Jeffrey, R Chandwani, EP Papapetrou, M Sadelain, D O'Carroll and EC Lai. (2010). Conserved vertebrate mir-451 provides a platform for Dicer-independent, Ago2-mediated microRNA biogenesis. Proc Natl Acad Sci U S A 107:15163–15168.
32. Cifuentes D, H Xue, DW Taylor, H Patnode, Y Mishima, S Cheloufi, E Ma, S Mane, GJ Hannon, *et al.* (2010). A novel miRNA processing pathway independent of Dicer requires Argonaute2 catalytic activity. Science 328:1694–1698.
33. Cheloufi S, CO Dos Santos, MMW Chong and GJ Hannon. (2010). A dicer-independent miRNA biogenesis pathway that requires Ago catalysis. Nature 465:584–589.
34. Ebert MS and Sharp PA. (2012). Roles for microRNAs in conferring robustness to biological processes. Cell 149: 515–524.

Address correspondence to:
Steven F. Dowdy, PhD
Department of Cellular and Molecular Medicine
UCSD School of Medicine
9500 Gilman Drive
La Jolla, CA 92093-0686

E-mail: sdowdy@ucsd.edu

Received for publication July 14, 2017; accepted after revision July 21, 2017.